Canadian Science Publishing

ARTICLE

Persistent impact of conventional seismic lines on boreal vegetation structure following wildfire

Quinn E. Barber, Christopher W. Bater, Anna Dabros, Jaime Pinzon, Scott E. Nielsen, and Marc-André Parisien

Abstract: Linear disturbances from geological exploration (i.e., seismic lines) have an extensive footprint across much of Canada's western boreal forest; however, how seismic lines interact with subsequent wildfire remains poorly understood. We assessed whether wildfires effectively mitigate the footprint of seismic lines by promoting forest recovery. We evaluated the forest structure of legacy seismic lines burned in 2001 and 2002 by comparing them against adjacent unburned control plots, using metrics derived from airborne laser scanning (ALS) data collected between 2007 and 2009. ALS metrics identified persistent differences in vegetation height and structure between seismic lines and adjacent forest controls, 7–9 years post-fire. Median canopy height was 2.90 m lower on upland seismic lines and 1.94 m lower on lowland seismic lines than on adjacent controls, corresponding to a 21% and 25% height reduction, respectively. Field surveys revealed greater graminoid and nonvascular plant cover, and lower tall-tree cover and dead vegetative matter, on seismic lines, in comparison with controls. Our results show that tree recovery remains significantly delayed on most upland and lowland burned seismic lines in our study area, and that additional management efforts or longer timescales may be required to restore these fragmented landscapes.

Key words: seismic lines, wildfire, boreal, lidar, airborne laser scanning.

Résumé : Les perturbations linéaires associées à l'exploration géologique (c.-à-d. les lignes sismiques) ont une vaste empreinte dans une grande partie de la forêt boréale de l'ouest du Canada. Cependant, on comprend mal de quelle façon les lignes sismiques interagissent par la suite avec les feux de forêt. Nous avons évalué si les feux de forêt atténuent effectivement l'empreinte des lignes sismiques en favorisant la récupération de la forêt. Nous avons évalué la structure de la forêt laissée en héritage par des lignes sismiques qui ont brûlé en 2001 et 2002 en les comparant à des parcelles témoins adjacentes non brûlées, à l'aide de mesures dérivées de données de balayage laser aéroporté (BLA) recueillies entre 2007 et 2009. Les mesures obtenues par BLA ont permis d'identifier des différences persistantes dans la hauteur et la structure de la végétation entre les lignes sismiques et les parcelles témoins adjacentes, 7 à 9 ans après le feu. La hauteur médiane du couvert forestier était 2,90 m plus courte dans les lignes sismiques des hautes terres et 1,94 m plus courte dans les lignes sismiques des basses terres que dans les témoins adjacents; ce qui correspond à une réduction de la hauteur de respectivement 21 et 25 %. Des relevés de terrain ont révélé la présence d'un couvert plus important de plantes non vasculaires et graminiformes, ainsi qu'un couvert moins important de grands arbres et de matière végétale morte dans les lignes sismiques, comparativement aux témoins. Nos résultats montrent que la récupération des arbres est significativement décalée dans les lignes sismiques brûlées sur les hautes et basses terres dans notre zone d'étude, et que des efforts additionnels d'aménagement ou des délais plus longs pourraient être nécessaires pour restaurer ces paysages fragmentés. [Traduit par la Rédaction]

Mots-clés : lignes sismiques, feu de forêt, boréal, lidar, balayage laser aéroporté.

1. Introduction

The North American boreal forest is a fire-adapted environment characterized by large, high-intensity wildfires often exceeding 100 000 ha in size (Stocks et al. 2002). These fires act as the primary agent of forest disturbance and a major driver of ecological diversity (Burton et al. 2008), affecting patterns of longevity and succession across a suite of fire-adapted species (Johnstone and Chapin 2006). Fire facilitates regeneration of vegetation communities through a variety of mechanisms, including removal of understory competition, canopy opening, mineral soil exposure, soil fertilization, and activating serotinous and semi-serotinous seed banks (Grier 1975; Ilisson and Chen 2009). Boreal fires are typified by high tree mortality (Johnstone et al. 2004) and rapid post-fire seedling recruitment (Greene et al. 1999), resulting in landscape mosaics of different even-aged forest stands. Variation in burn severity and pre-fire species composition affect post-fire seedling recruitment rates and ultimately define post-fire species assemblages (Whitman et al. 2018; Johnstone et al. 2020).

Wildfires burning in the Canadian boreal forest frequently encounter anthropogenic features, including those related to resource development from the forestry and energy industries. This includes seismic lines: long, narrow corridors intended for the exploration of underground oil and gas reserves using

Received 20 October 2020. Accepted 2 April 2021.

Q.E. Barber, A. Dabros, J. Pinzon, and M.-A. Parisien. Northern Forestry Centre, Canadian Forest Service, Natural Resources Canada, 5320 122 Street NW, Edmonton, AB T6H 3S5, Canada.
C.W. Bater. Forest Stewardship and Trade Branch, Forestry Division, Alberta Agriculture and Forestry, Suite 303, 7000 - 113 Street, Edmonton, AB T6H 5T6, Canada.
S.E. Nielsen. Department of Renewable Resources, University of Alberta, 751 General Services Building, Edmonton, AB T6G 2H1, Canada.
Corresponding author: Quinn E. Barber (email: quinn.barber@canada.ca).

seismic waves (Dabros et al. 2018). The province of Alberta hosts extensive resources development, including the highest number of seismic lines in Canada, with densities sometimes exceeding 10 km·km^{-2} (Lee and Boutin 2006). Much of the environmental impact comes from so-called conventional seismic lines, which are approximately 5–10 m wide and were constructed until the mid-1990s, after which a new practice of constructing low-impact seismic lines consisting of tightly spaced 2- to 4-m-wide clearings was introduced (Dabros et al. 2018). The construction of conventional seismic lines was typically done with heavy tracked machinery, resulting in topsoil removal and soil compaction (Bliss and Wein 1972).

Until recently, seismic lines were rarely restored and often failed to regenerate naturally (van Rensen et al. 2015), contributing to a suite of persistent environmental impacts such as an influx of non-native and disturbance-tolerant species (Honnay et al. 2002; Finnegan et al. 2018*a*), increased human recreational access (Pigeon et al. 2016), and changes in biodiversity from habitat alteration (Riva et al. 2018, 2020). The decline of woodland caribou (*Rangifer tarandus caribou*), a nationally threatened species, has been directly connected to the fragmentation of the boreal forest by these seismic lines (Latham et al. 2011; DeMars and Boutin 2018). Van Rensen et al. (2015) reported that at least one third of previously forested lines would fail to recover to 3 m vegetation height without human intervention, even after 50 years, whereas Lee and Boutin (2006) reported only 8.2% of seismic lines recovered to 50% woody vegetation cover 35 years after disturbance. Where it occurs, passive recovery (as opposed to human intervention) on seismic lines is often stunted (Revel et al. 1984), and understory community development is considerably delayed (Finnegan et al. 2019). Restoring microtopography and reducing access (e.g., by felling trees onto the seismic lines) are two common methods of seismic line restoration, albeit with no guarantee of success (Stevenson et al. 2019; Echiverri et al. 2020).

Wetlands of the western boreal forest are particularly sensitive to the construction of linear features. Seismic line construction causes soil compaction leading to elevated soil moisture content (Dabros et al. 2017; Pinzon et al. 2021), which hinders vegetation recovery, particularly in lowland areas (Lee and Boutin 2006; van Rensen et al. 2015). This compaction occurs as a function of soil type, pre-disturbance soil moisture, water table depth, and the time of year of seismic line construction (Dabros et al. 2018). Minimal long-term effects may be observed on sandy soils or gravel (Bliss and Wein 1972), but finer-textured mineral soils or the organic soils of peatlands frequently experience lasting degradation (Camill et al. 2010; van Rensen et al. 2015; Dabros et al. 2017).

Given the transformative effects of wildfire, there is speculation that wildfire on seismic lines could act as a form of passive restoration, but there is divergent and limited evidence to support this assertion. Vegetation recovery appears to be accelerated by wildfire in bogs, poor mesic forests, and uplands dominated by jack pine (*Pinus banksiana* Lamb.), but it lags on other sites such as fens and sites lacking microtopography (Filicetti and Nielsen 2018, 2020). Pinzon et al. (2021) reported that the seismic line footprint persisted through intense wildfire, as evidenced by differences in soil volumetric water content, canopy cover, snag density, and plant and arthropod assemblages between burned seismic lines and burned forest. New methods are needed to monitor seismic lines quickly and across large areas, so land managers can better prioritize the places where restorative measures are most needed to reset the ecosystem on its expected (or desired) succession trajectory.

Assessing seismic line recovery can be costly and logistically difficult given the remoteness and extent of seismic line networks (Dabros et al. 2018). Airborne laser scanning (ALS) has grown in popularity for its ability to provide landscape-scale data related to forest structure, including vegetation height and stem volume (Næsset et al. 2004; Vastaranta et al. 2011). ALS may be employed in monitoring forest condition following harvest (Wulder et al. 2008) and wildfire (Bolton et al. 2015), both achievable objectives even with the low-density ALS data commonly collected in the 2000s (Næsset et al. 2004; Debouk et al. 2013). The availability of ALS data provides an excellent opportunity to assess the state of the aging network of conventional seismic lines in Alberta on a large scale, without establishing expensive and often logistically difficult field campaigns. Two studies in Alberta have examined seismic line recovery using ALS, with both finding that seismic lines had reduced tree height when compared with nondisturbed forests (van Rensen et al. 2015; Finnegan et al. 2018*b*); however, neither study explicitly assessed burned seismic lines and whether wildfire promoted or hindered vegetation recovery.

The objectives of this study were to (*i*) use ALS to determine whether conventional seismic lines, having experienced high-intensity fire, were recovering to a vegetation height and structure similar to that of adjacent forests, and (*ii*) test the usefulness of an extensive ALS dataset for complementing post-fire recovery field surveys. In this study, we used ALS data to assess seismic line recovery following fire at two locations in north-central Alberta's boreal forests. We compared seismic lines against adjacent forest control plots within the footprint of two large wildfires, explicitly selecting burned conventional seismic lines.

2. Methods

2.1. Study area

The study area is located in north-central Alberta in the Boreal Plain ecozone, which can be broadly divided into drier uplands and wetter lowlands. Dominant tree species include trembling aspen (*Populus tremuloides* Michx.), white spruce (*Picea glauca* Moench (Voss)), and jack pine on uplands, interspersed with black spruce (*Picea mariana* (Mill.) B.S.P.) and eastern larch (*Larix laricina* (Du Roi) K. Koch) in wetlands (hereinafter "lowlands") (Ecological Stratification Working Group (ESWG) 1996). These areas are used by both the oil and gas and forestry industries, leading to the presence of many anthropogenic features such as seismic lines, pipelines, well pads, steam-assisted gravity drainage oil extraction plants, cut blocks, and access roads (ABMI 2018). Surficial geology for the region is composed of a mix of glaciofluvial and glaciolacustrine deposits, and organic peatland soils (Fenton et al. 2013). These peatland soils are entirely organic and are found in lowlands, which are characterized by very slow water movement (Pennock and Sanborn 2015). The boreal forest in the province of Alberta burns at a rate between 0.09% and 2.20% annually (Tymstra et al. 2005). The Chisholm wildfire burned an area in north-central Alberta of approximately 110 000 ha in May 2001. The fire was driven by winds of 50 km·h^{-1}, gusting to 80 km·h^{-1}, and was characterized by extreme intensity, burning up to 225 000 kW·m^{-1}. The fire caused near-complete overstory mortality and destroyed the small community of Chisholm, stopping short of the town of Slave Lake (Alberta Sustainable Resource Development 2001). The House River wildfire burned an area of approximately 248 000 ha in northeastern Alberta in May 2002, under similar conditions to the Chisholm wildfire (Tymstra et al. 2002). Winds exceeded 30 km·h^{-1}, driving the fire through stands of black spruce, trembling aspen, jack pine, eastern larch, and extensive lowlands. Both the Chisholm and House River fires burned over areas with relatively high densities of seismic lines: 2.42 and 1.99 km·km^{-2}, respectively (ABMI 2018).

2.2. Sample plot selection

Test plots were randomly selected from conventional seismic lines, identified in the Alberta Biodiversity Monitoring Institute (ABMI) Human Footprint Inventory (ABMI 2018). Each test plot was 100 m long and 6 m wide. For each sample plot, two candidate control plots were offset 50 m from each side of the line into

Fig. 1. Field photographs representing typical site conditions for uplands and lowlands, seismic line plots and control plots. [Colour online.]

the adjacent forest. We evaluated if candidate control plots and corresponding sample plots were in the same upland and lowland regimes (Fig. 1) using the ABMI Boreal Wetland Probability dataset (DeLancey et al. 2019); only matching candidate control plots were retained, and if both candidate control plots met this criterion, one was randomly selected. If neither control plot matched the sample plot upland or lowland regime, that sample was dropped. We generated 1500 sample per control plot pairs within each of the Chisholm and House River fire perimeters, and an additional 1500 unburned sample and control plot pairs within 20 km of each of the Chisholm and House River fire perimeters (Fig. 2). Our paired sample design (i.e., dependent samples) allowed us to control for the effects of spatial variability in site conditions (moisture, topography, soil type, etc.) and plant communities.

Conventional seismic lines were constructed with little regard for topography, vegetation, or wetlands (Dabros et al. 2018). This lends itself to paired control plots positioned adjacent to seismic lines, given that a control plot will almost always be in the same topoedaphic setting as its paired seismic-line plot. We filtered our random plots using the following criteria: plots were located a minimum of 50 m from roads, 100 m from mapped waterbodies, 1 km from highways, and 4 km from communities; plots were not impacted by recorded harvesting or wildfire more recent than 1950, other than the Chisholm or House River fires; and plots were located at least 50 m from one another. All plot generation and selection was performed in R version 4.0.3 (R Core Team 2020).

Site selection involved the use of several secondary spatial datasets, such as maps of access features, which are listed in Appendix Table A1. We checked randomly generated plot locations using Bing Maps aerial imagery (https://www.bing.com/maps; Microsoft 2019 to confirm that seismic lines had been correctly classified in the human footprint dataset (Appendix B). We calculated mean difference normalized burn ratio (a measure of fire severity, dNBR; Key and Benson 2006) from pre- and post-fire Landsat satellite imagery, removing any plots below a threshold of 100, which corresponds to a minimum of low-severity fire (Parks et al. 2014). After filtering any sites with insufficient ALS coverage, 2070 plot pairs were retained: 574 within the Chisholm fire boundary, 483 within 20 km of the Chisholm fire, 490 within the House River fire boundary, and 523 within 20 km of the House River fire.

2.3. Airborne laser scanning data analysis

ALS vegetation metrics were generated by the Government of Alberta's Department of Agriculture and Forestry, using low-density (1.4 returns·m^{-2} (Appendix Table A1)) point cloud data collected between 2007 and 2009 (Appendix A). Point clouds were

Fig. 2. Study area and in-fire seismic line plots, including Chisholm fire (A) and House River fire (B) of central Alberta, Canada. Basemap is a hillshade of the NASA SRTM 30 m digital elevation model (Farr et al. 2007). Produced in QGIS 3.10 (QGIS.org 2019). [Colour online.]

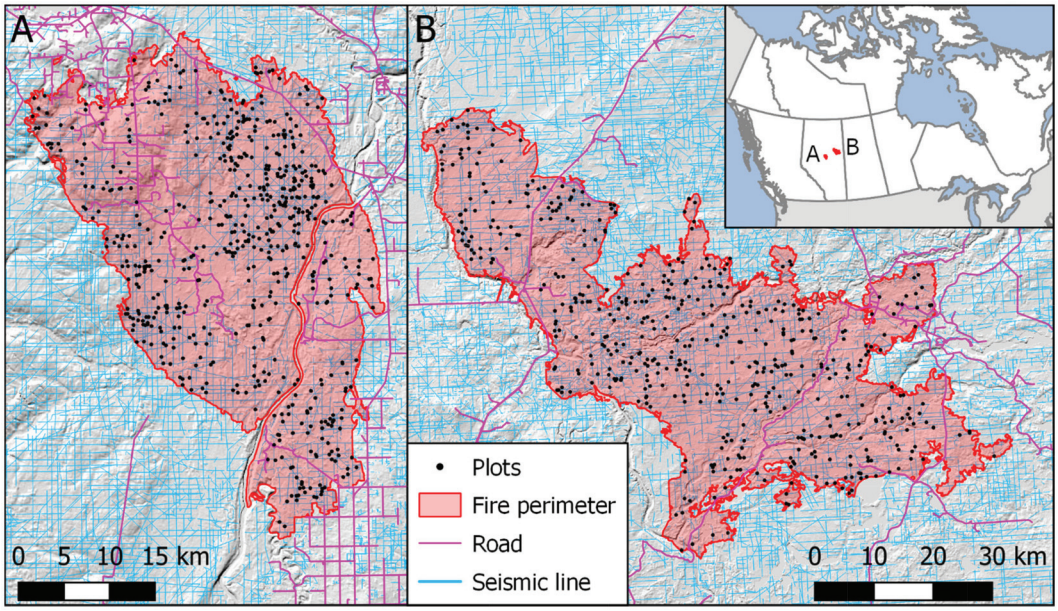

Table 1. Airborne laser scanning derived vegetation metrics.

Variable	Description
$Height_{P05}$	5th percentile return height (m)
$Height_{P10}$	**10th percentile return height (m)**
$Height_{P25}$	25th percentile return height (m)
$Height_{P50}$	50th percentile return height (m)
$Height_{P75}$	75th percentile return height (m)
$Height_{P95}$	95th percentile return height (m)
$Height_{P99}$	**99th percentile return height (m)**
$Height_{mean}$	**Mean return height (m)**
$Height_{variance}$	Return height variance
$Height_{kurtosis}$	Return height distribution kurtosis
$Height_{skewness}$	**Return height distribution skewness**
Canopy return ratio	Ratio of mean height over maximum height
% $returns_{>0.15\ m}$	Proportion of returns greater than 0.15 m
% $returns_{0.15–2.00\ m}$	Proportion of returns 0.15–2.0 m
% $returns_{2.00–5.00\ m}$	Proportion of returns 2.0–5.0 m
% $returns_{5.00–10.00\ m}$	Proportion of returns 5.0–10.0 m
% $returns_{10.00–30.00\ m}$	Proportion of returns 10.0–30.0 m
% $returns_{>2.00\ m}$	**Proportion of returns greater than 2.0 m**

Note: Bolded metrics were retained for figures and statistical analysis.

Table 2. Linear regression model results evaluating the effect of wetland class, seismic line class, CTI, dNBR, and distance to road on 99th percentile vegetation height.

Variable	Std. coeff.	Std. error	*t* value	*p* value	% contribution
Intercept	8.702	0.549	15.910	<0.001	—
UPLAND	3.255	0.781	4.189	0.009	44.3
SEISMIC	−2.230	0.638	−3.502	0.010	30.4
CTI	−1.031	0.399	−2.601	0.066	14.0
dNBR	0.592	0.351	1.695	0.177	8.0
ROADDIST	−0.244	0.324	−0.761	0.412	3.3

Note: Models were built on a random 10% of the burned plots (218 plots), repeated 100 times and averaged. The % contribution indicates percent variance explained by each variable, calculated as proportion of the sum of all standardized coefficients. UPLAND, upland–lowland dichotomous class; SEISMIC, seismic line presence or absence as a dichotomous class; CTI, compound topographic index (as a continuous measure of meso-scale terrain wetness); dNBR, differenced normalized burn ratio (continuous fire severity); ROADDIST, distance to road (as an approximation of potential use of seismic lines by people).

processed into height metrics using FUSION software (McGaughey 2009), based on the distribution of return heights within sample plots (Appendix Fig. A1). We built a canopy height model at a spatial resolution of 2 m for visualization (Fig. A1). Calculating vegetation metrics involved normalizing ALS returns to height above ground level and processing these into a suite of summary statistics characterizing height, structure, and cover. From an initial dataset of 165 ALS metrics, we discarded those that were not reproducible or might be considered statistical outliers (such as maximum return height or return intensity metrics; Bater et al. (2011)), and metrics that were not relevant to our research question (such as total return count), resulting in 18 candidate metrics (Table 1). From these, we identified and removed correlated variables ($|r_{spearman}| \geq 0.7$). When choosing between a pair of correlated variables, we retained variables that had been reported in related literature, and otherwise selected from pairs to maximize the number of retained variables. This resulted in the retention of six structural vegetation metrics: 10th percentile return height ($Height_{P10}$), 75th percentile return height ($Height_{P75}$), 99th percentile return height ($Height_{P99}$), mean return height ($Height_{mean}$), return height distribution skewness ($Height_{skewness}$), and proportion of returns greater than 2.0 m (% $returns_{>2.0\ m}$). Mean return height has been frequently reported as useful by others (van Rensen et al. 2015; Finnegan et al. 2018*b*) and therefore was included despite being positively correlated with ($Height_{P75}$).

We compared measures from the selected vegetation metrics between seismic line plots and control plots in both burned and unburned sites using paired Wilcoxon rank-sum tests, grouped by lowland and upland (Table 2). We opted for this nonparametric test because the data were non-normal (Shapiro–Wilk test, $p < 0.0001$). The interpretation of ALS metrics depends on their area-specific context. For example, $Height_{P75}$ may be interpreted as a measure of approximate stand height, assuming that ALS responses are not heavily influenced by small-scale forest gaps or other disturbances (Drake et al. 2002; Bolton et al. 2015), and % $returns_{>2.0\ m}$ is correlated with canopy cover (Bolton et al. 2015). $Height_{P75}$ and $Height_{mean}$ are also correlated with total

aboveground biomass (Drake et al. 2002; Bolton et al. 2015). $Height_{skewness}$ and $Height_{kurtosis}$, which describe the shape of the ALS return distribution, depend on residual snags (standing dead trees) and the timing of recovery. For example, high kurtosis may be associated with strong even-aged recovery (Bolton et al. 2015). Van Rensen et al. (2015) used maximum return height to define top-of-canopy height, while we used $Height_{P99}$ to avoid the effect of outliers. We also tested if it was appropriate to pool the Chisholm and House River fire plots by comparing the six selected ALS metrics between fires using a Wilcoxon rank-sum test.

We fit a linear regression model of vegetation height to explore the importance of seismic lines compared to other environmental factors and to evaluate whether stratification into upland or lowland was necessary. We modelled vegetation height using a response variable of vegetation height ($Height_{P99}$), excluding all unburned sites from out modelling. Our explanatory variables included four environmental spatial datasets and one site history variable: compound topographic index (CTI, aka topographic wetness index) as a continuous measure of meso-scale terrain wetness, distance to road (ROADDIST) as an approximation of potential use of seismic lines by people, upland–lowland dichotomous class (UPLAND), seismic line presence or absence as a dichotomous class (SEISMIC), and continuous fire severity (dNBR, Key and Benson 2006). CTI was calculated from a 15 m resolution ALS-derived digital elevation model, and ROADDIST was based on Natural Resources Canada CanVec Transportation dataset (Natural Resources Canada 2019) (details in Appendix Table A4). To avoid false significance caused by a large sample size and account for spatial dependence in the data, we fit 100 models on random 10% subsets of our plot data, sampling without replacement. These 100 independent models were then averaged (Table 2). Spatial autocorrelation in model residuals was insignificant at this sample size (Global Moran's I statistic, $p = 0.199$). Model residuals were normal, and the variance was homogeneous. All modelling was performed in R version 4.0.3 (R Core Team 2020).

2.4. Field validation

In the summer of 2018, we conducted field reconnaissance of 22 locations (11 for each fire). Sites were randomly selected from our ALS plot dataset, including only sites that were within 1 km of access roads and were accessible by foot. Field observations of vegetation cover (%) of different functional groups and vegetation structure were taken on 20 m long × 6 m wide subplots nested within the seismic line plot (100 m long × 6 m wide) and a parallel 20 m × 6 m subplot nested within the control plot. Each subplot was divided into four 5 m sections, within which a 1 m^2 quadrat was randomly placed, approximately equidistant from the seismic line edges. Quadrats were used to estimate the percent cover of functional groups including low shrubs (≤1.5 m, including low and creeping shrubs), tall shrubs (>1.5 m), short trees (1–5 m), tall trees (>5 m), forbs, graminoids (grasses, sedges), nonvascular (mosses, liverworts), and percent cover of dead vegetation. Percent cover was averaged per subplot and a Wilcoxon rank-sum test was performed to evaluate differences. We collected additional field data (e.g., seismic line width, presence of snags, evidence of human or wildlife use, and identification of dominant vascular plant species), intended primarily for validation and better knowledge of site conditions and characteristics. In cases where ALS plots were inaccessible by foot, subplots were moved closer to the road to make foot access feasible, without changing the individual seismic line being investigated.

3. Results

Vegetation height and structure were significantly different between paired seismic lines and control plots (Figs. 3, A2) for all six selected metrics (paired Wilcoxon rank-sum test, $p < 0.0001$). Comparing the median of burned seismic line plots and burned control plots, $Height_{P75}$ was lower on seismic lines than control plots ($\Delta = -0.81$ m), with greater difference in upland plots ($\Delta = -0.74$ m) than lowland plots ($\Delta = -0.595$ m). Top-of-canopy height ($Height_{P99}$) was higher on control plots than seismic lines ($\Delta = -2.74$ m), and this effect was also stronger in upland plots ($\Delta = -2.90$ m) than in lowland plots ($\Delta = -1.94$ m). This corresponds to a relative height reduction of 21% and 25% in uplands and lowlands, respectively. Canopy cover, as estimated by % $returns_{>2.00\ m}$, was also higher on control plots for both upland ($\Delta = -7.6\%$) and lowland ($\Delta = -4.1\%$) plots. Lower $Height_{mean}$ for seismic lines ($\Delta = -0.57$ m) corresponded to lower or more open vegetation in general when compared to adjacent control forests. All differences in medians were significant ($p < 0.001$) for both lowlands and uplands, with the exception of % $returns_{0.15–2.00\ m}$ in uplands, pointing to lower overall vegetation height and density on lines.

Stand height was more variable (from $Height_{variance}$) for control plots than for seismic lines, with greater variability in uplands than in lowlands (Appendix Table A2), whereas $Height_{skewness}$ and $Height_{kurtosis}$ were higher on seismic lines. This is likely indicative of continuous low vegetation on seismic lines compared to variable, sometimes tall tree growth on control plots. Canopy closure, as estimated from % $returns_{>2.00\ m}$ and $Height_{variance}$, was low for both control plots and seismic line plots. These patterns of taller vegetation on control plots persisted for plots outside of the fire perimeter (Appendix Fig. A2), although vegetation in unburned areas was taller on average (Appendix Fig. A3). Comparing the Chisholm sites and the House River sites, we found no significant differences in any of six metrics considered in this study (paired Wilcoxon rank-sum test, $p < 0.05$), allowing us to pool the data from the two study areas.

Regression modelling indicated that UPLAND had the strongest effect on vegetation height, contributing 44.3% of the variance explained (Table 2), based on standardized model coefficients. SEISMIC was the second most important variable, contributing 30.4% of the variance explained. The other variables did not achieve significance ($p < 0.05$), although CTI was almost significant ($p = 0.06$), contributing 14.0% of the variance explained. Model coefficients were positive for lowland class, negative for seismic line class, and negative for CTI, indicating taller vegetation in uplands, control plots, and drier sites, respectively. The adjusted R^2 was 0.29.

While being cautious of the low sample size, field observations provided further support for differences between conventional seismic lines and adjacent forests (Fig. 4). Seismic line field plots had greater cover of nonvascular plants and graminoids ($\Delta = +7.8\%$ and $\Delta = +15.6\%$, respectively) than field control plots. Further, seismic lines exhibited lower percent cover of dead vegetative matter ($\Delta = -19.2\%$) and low shrubs ($\Delta = -7.9\%$), and lower density of trees greater than 5 m in height ($\Delta = -32.9\%$) (Fig. 4). Ground plot sample sizes were too small to meaningfully compare lowland seismic line plots against lowland control plots ($n = 6$), but this comparison could be carried out for upland field plots ($n = 16$). Upland seismic lines had significantly higher graminoid cover ($\Delta = +17.7\%$), lower cover of dead vegetative matter ($\Delta = -23.4\%$), and lower cover of trees greater than 5 m in height ($\Delta = -42.9\%$) compared with control plots. No obvious signs of human use were present. We observed game trails on or adjacent to 86% of seismic line field plots, and only 14% of control field plots. Snags were rare across all field sites, except for three control lowland field plots, where dead wood (standing and fallen) represented approximately 5% of total plot area.

4. Discussion

4.1. Legacy of seismic lines on vegetation structure

Past seismic line construction affected present vegetation height, secondary only to lowland–upland class among the variables considered. This illustrates the significant and lasting impact that seismic lines have on forest structure, an impact that was not mitigated by intense wildfire. ALS metrics indicated shorter, more

Fig. 3. Comparison of selected airborne laser scanning statistics between burned seismic lines and paired control plots (n = 1064), grouped by upland (orange) and lowland (blue). Boxes represent the 25th, 50th, and 75th percentiles (quartiles). Whiskers represent the lowest (highest) datum within 1.5 times the interquartile range (third - first quartile) of the first (third) quartile. All comparisons between seismic lines and controls are statistically significant ($p < 0.0001$, paired Wilcoxon rank-sum test, Table A2). [Colour online.]

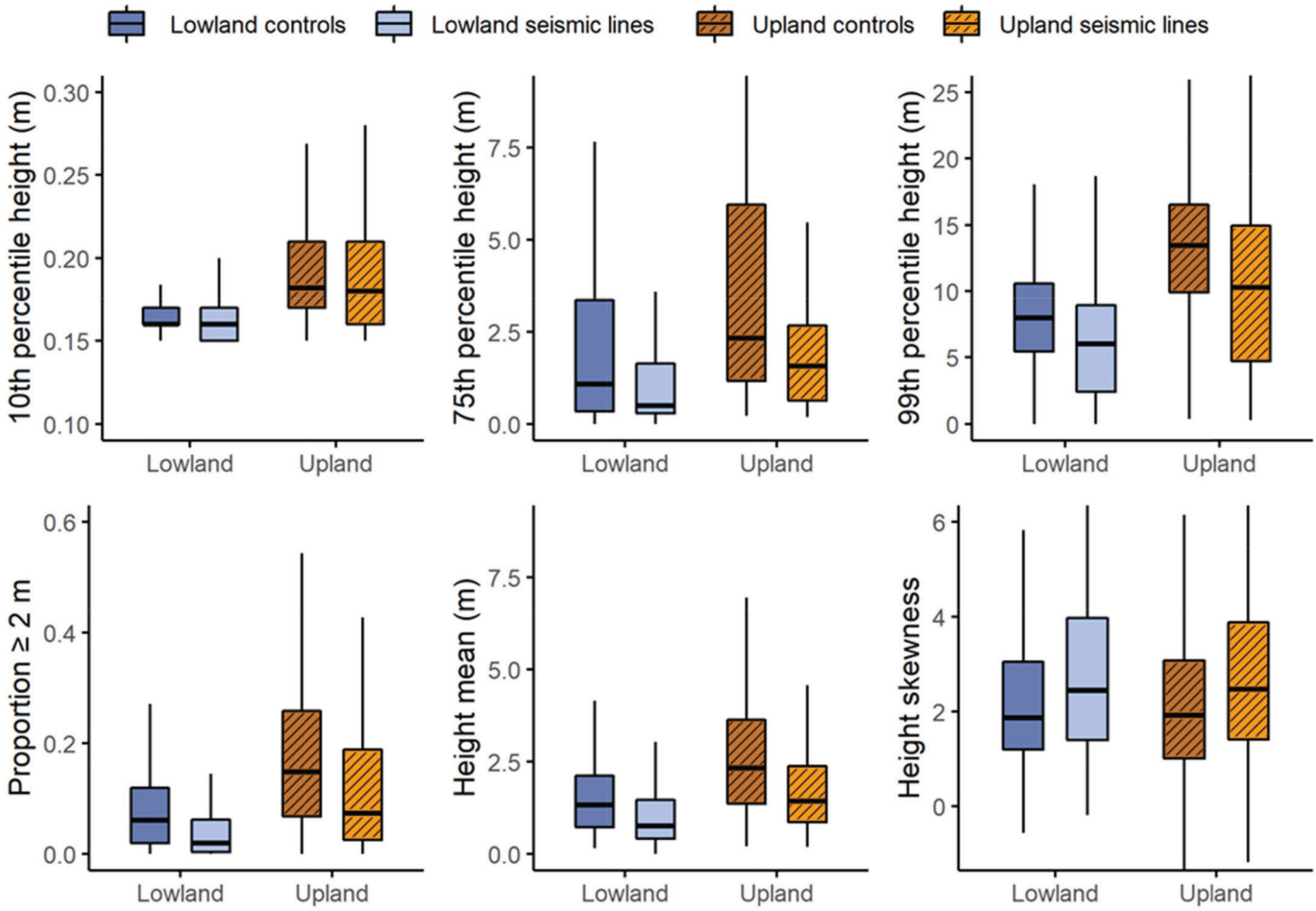

open vegetation in both lowland and upland seismic line sites, translating to a deficit of aboveground biomass (Bolton et al. 2015; Drake et al. 2002) relative to adjacent control plots. Seismic lines possessed a more open canopy, a lower density of trees, and a greater cover of nonarboreal vegetation. These results reaffirm that burned seismic lines are often associated with slower vegetation growth or establishment failure in the western boreal forest, contributing to the existing problem of seismic lines dominated by disturbance-associated species that are often invasive or exotic (Honnay et al. 2002; Finnegan et al. 2018*a*).

ALS return height distribution skewness and kurtosis were higher on seismic line plots than in corresponding control plots. This suggests a relatively uniform height, such as graminoids in lowland plots or tall deciduous shrubs in upland plots, without successional tree recovery. Although high kurtosis may also be associated with strong, uniform recovery (age) of woody species (as in Bolton et al. 2015), this was not observed during our field visits. Seismic line forest canopies were frequently open or entirely absent, as indicated by lower proportion of returns greater than 2 m. The observed rarity of snags suggests that these had little impact on ALS metrics, although it is possible that snags were present during ALS collection and had since fallen. Reduced biomass in seismic lines may affect future fire behaviour, acting as *de facto* fuel treatment as suggested in Deane et al. (2020), a "compound interaction" (Buma 2015) between the subsequent disturbances, which further limits wildfire's ability to restart succession.

Previous studies have documented that upland seismic lines regenerate considerably faster than lowland sites, possibly due to their greater resiliency (defined as the ability of an ecosystem to return to a previous state following a disturbance effect; Elmqvist et al. (2003)) to seismic line disturbance and faster growth of early successional trees (Revel et al. 1984; Lee and Boutin 2006; van Rensen et al. 2015). However, we observed that upland and lowland seismic lines had a similar reduction in vegetation height relative to control plots, 21% and 25%, respectively (Appendix Table A2; Fig. A4). This indicates that some upland sites are not recovering as might be expected. The relative height reduction on burned seismic lines was greater than on unburned seismic lines (Appendix Table A3), further reinforcing that fire has not led to recovery of these seismic lines seven to nine years post-fire. It may be that there are variable soil and vegetation conditions across upland sites, some of which impart resiliency to disturbance. This would parallel lowlands, where wildfire appears to aid seismic line recovery in some wetland types but not others (Filicetti and Nielsen 2020).

During field visits we observed a lack of trees over 5 m tall on seismic lines, even when tall trees were abundant on control sites. Instead, seismic lines were generally populated with trees under 5 m, nonvascular plants, and abundant graminoids, including

Fig. 4. Percent cover of functional groups of vegetation observed during field validation of a select sample (n = 22) of paired field plots. Dots represent median cover percentages, whiskers represent 95% confidence intervals. p values are coded symbolically (*, $p \leq 0.05$; **, $p \leq 0.01$; ***, $p \leq 0.001$; ****, $p \leq 0.0001$: paired Wilcoxon rank-sum test). [Colour online.]

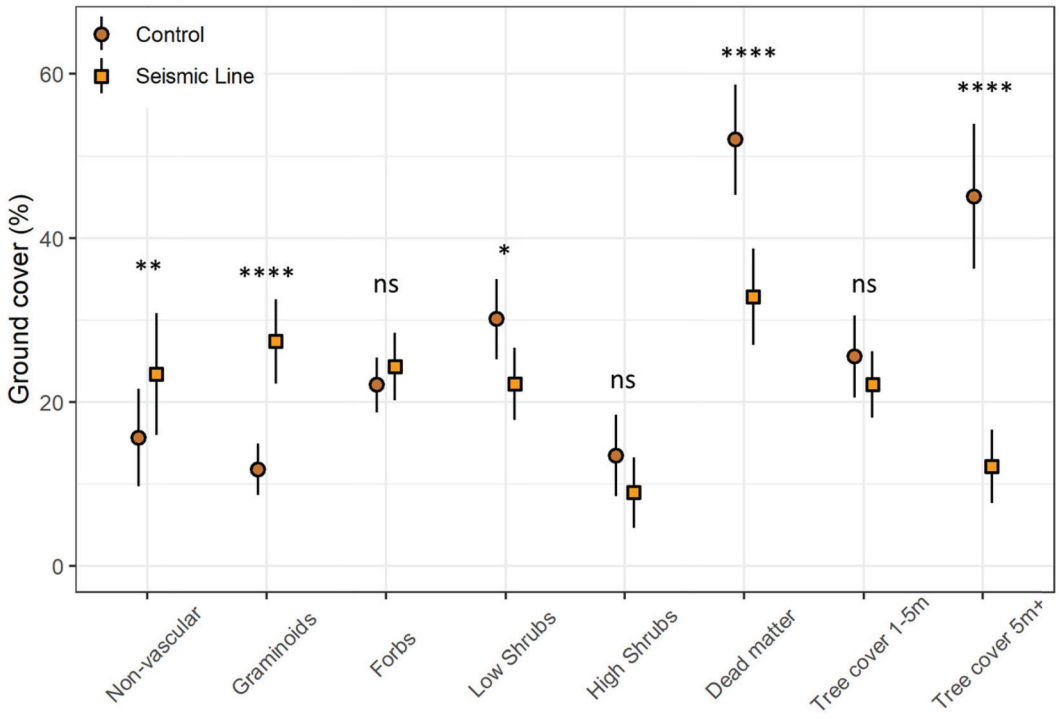

upland and lowland sites. These results are consistent with studies comparing conventional seismic lines to adjacent, undisturbed forest, which found vegetation height below 2 m on seismic lines, as well as occasional failure to recover past a low shrub and herbaceous understory (Lee and Boutin 2006; Finnegan et al. 2019). A parallel can be drawn between this and the combined disturbance of wildfire and forest harvest, where areas of overlapping fire and harvest experienced a tree species shift from coniferous to deciduous species (Bouchard and Pothier 2011). Our field results must be interpreted with caution, given the low sample size and lack of spatial coverage of our field plots. These field visits did serve their purpose, as they allowed us to not only corroborate but also refine our understanding of the differences recorded by the aerial surveys.

4.2. Implications

We assessed a large number of sites using ALS, which would have been prohibitively expensive and logistically unfeasible using traditional field surveys. ALS plots were selected in a comparatively unbiased manner, alleviating the bias by accessibility usually associated with field studies. While our ALS plots were useful for measuring vegetation height and structure, they provide a rather coarse estimate of seismic line recovery compared to traditional field-based regeneration surveys. There have been several efforts to model regeneration density with low-density ALS, but in general model predictions of stem number are poor (Næsset et al. 2004). As such, field-proofing is indispensable for verifying observations and validating conclusions based on ALS data. The critical need for field-proofing is best exemplified here by our observations ruling out excessive human access, and it also provides an on-the-ground context to ALS metrics.

Poor tree regeneration following fire in seismic lines will have ecological consequences, notably for the nationally endangered boreal woodland caribou. Increased moisture on seismic lines decreases the severity of subsequent wildfire within seismic lines, or alternately allows wildfire to "skip" over seismic lines, creating distinct ecological communities within the post-fire seismic line footprint (Pinzon et al. 2021). For example, Riva et al. (2020) found that burned seismic lines fostered many plant and butterfly species that use these early seral spaces. From our own observations, game trails were nearly ubiquitous on our seismic line field plots, providing further evidence that in our study area these features are being used as wildlife movement corridors even when partially regenerated. This likely includes the use of seismic lines by gray wolves (*Canis lupis*), who use these access pathways in pursuit of prey, leading to their incidental predation of caribou (Latham et al. 2011; DeMars and Boutin 2018). In particular, wolves have been found to move more quickly on seismic lines with mean vegetation height less than 0.7 m (Finnegan et al. 2018*b*), which includes many of our sites.

While we found no evidence that wildfire triggers or accelerates seismic line vegetation recovery, Filicetti and Nielsen (2018) reported strong post-fire jack pine regeneration along seismic lines. They suggest that site recovery is related to pre-fire species composition and site conditions, such as ecotype, soil type, and moisture regime. Jack pine is particularly fire adapted among boreal tree species, as it depends on fire to activate its serotinous cones, and to expose mineral soil through burning of organic matter (de Groot et al. 2004). Given this dependence on fire and its shade intolerance (Claveau et al. 2002), jack pine could be expected to benefit from both seismic line construction and wildfire in some instances. In a related study, Filicetti and Nielsen (2020) showed that wildfire on seismic lines promoted regeneration of serotinous species, including jack pine and black spruce, but that increasing terrain wetness (or conversely, decreasing depth to water table) negatively correlated with regeneration density.

4.3. Scope and limitations

The advantages of remote sensing come with material trade-offs. Low-density ALS point clouds are not appropriate for species

classification; therefore, our height measurements undoubtedly responded to tall deciduous shrubs or overhanging canopies from seismic line edges, and we lacked the ability to stratify by species. Through low-density ALS alone, it difficult to obtain certain forest mensuration estimates, such as the number of established trees (Næsset et al. 2004). Direct seedling counts and tree diameter measurements would be a more relevant measure of forest successional stage, as would species identification; however, these are costly and time consuming to measure and report across a large area. Methods for counting seedlings using drones show promise (Fromm et al. 2019), but this may not be practical over the larger extent of disturbances. Our targeted field visits were designed to validate ALS plot location. Though limited, these field visits were important to rule out human use influencing our results and to provide on-the-ground context to ALS metrics, thereby helping us understand the nature of discrepancies in vegetation recovery. ALS data were collected between 2007 and 2009, and so comparison with our 2018 field measurements was necessarily qualitative. Given the limited nature of our field reconnaissance, we did not record tree stem counts or basal area.

We rely on the assumption that seismic lines and control plots are similar within pairs, which are the basis for our comparison, based on their being only 50 m apart and being located in the same upland or lowland ecosystem. Unaccounted-for differences, such as small-scale differences in soil type and moisture regime, may increase noise in the analysis. Pre-construction community composition is not reliably known. Further research is needed to evaluate how soil conditions, pre-disturbance vegetation communities, and site history variables affect regenerating seismic line recovery. However, our results clearly show that seismic line presence is an influential factor defining post-fire forest structure.

5. Conclusion

Given the fire-adapted species of the boreal forest, stand-renewing fire might be assumed to mitigate the footprint of seismic lines by initiating vigorous vegetation regeneration. In this study we found that wildfires do not "restore" seismic lines to vegetation trajectories under typical conditions found in the boreal forest of central Alberta. We found an average canopy height reduction of 21%–25% on seismic lines relative to adjacent forest plots, 7–9 years post-fire. The use of ALS allowed us to assess thousands of remote plots, whereas traditional field methods would have required either helicopter access or limited winter snowmobile surveys of unburied vegetation. Continued and widespread monitoring of the seismic line network will be necessary to ensure that the environmental effects associated with linear features are mitigated, either naturally or through managed reclamation.

Acknowledgements

This work was supported through research grants from the Office of Energy Research and Development, Natural Resources Canada through the Energy Innovation Program (project FF-OS-024). We thank Xianli Wang and Eric Neilson for assistance in the field and Evan R. DeLancey for assistance with the ABMI Wetland Inventory dataset. We thank Ellen Whitman for providing fire severity data.

References

ABMI. 2018. Human footprint inventory: wall-to-wall human footprint inventory. Alberta Biodiversity Monitoring Institute and Alberta Human Footprint Monitoring Program. Available from https://www.abmi.ca/home/data-analytics/da-top/da-product-overview/Human-Footprint-Products/HF-inventory.html [accessed 31 October 2019].

Alberta Sustainable Resource Development. 2001. Final Documentation Report, Chisholm Fire (LWF-063). Available from https://open.alberta.ca/publications/0778518418#summary [accessed 2 October 2019].

Bater, C.W., Wulder, M.A., Coops, N.C., Nelson, R.F., Hilker, T., and Næsset, E. 2011. Stability of sample-based scanning-LiDAR-derived vegetation metrics for forest monitoring. IEEE Trans. Geosci. Remote Sens. **49**(6): 2385–2392. doi:10.1109/TGRS.2010.2099232.

Bliss, L.C., and Wein, R.W. 1972. Plant community responses to disturbances in the western Canadian Arctic. Can. J. Bot. **50**(5): 1097–1109. doi:10.1139/b72-136.

Bolton, D.K., Coops, N.C., and Wulder, M.A. 2015. Characterizing residual structure and forest recovery following high-severity fire in the western boreal of Canada using Landsat time-series and airborne lidar data. Remote Sens. Environ. **163**: 48–60. doi:10.1016/j.rse.2015.03.004.

Bouchard, M., and Pothier, D. 2011. Long-term influence of fire and harvesting on boreal forest age structure and forest composition in eastern Québec. For. Ecol. Manage. **261**(4): 811–820. doi:10.1016/j.foreco.2010.11.020.

Buma, B. 2015. Disturbance interactions: characterization, prediction, and the potential for cascading effects. Ecosphere, **6**(4): 1–15. doi:10.1890/ES15-00058.1.

Burton, P.J., Parisien, M.-A.A., Hicke, J.A., Hall, R.J., and Freeburn, J.T. 2008. Large fires as agents of ecological diversity in the North American boreal forest. Int. J. Wildl. Fire, **17**(6): 754–767. doi:10.1071/WF07149.

Camill, P., Chihara, L., Adams, B., Andreassi, C., Barry, A., Kalim, S., et al. 2010. Early life history transitions and recruitment of *Picea mariana* in thawed boreal permafrost peatlands. Ecology, **91**(2): 448–459. doi:10.1890/08-1839.1.

Claveau, Y., Messier, C., Comeau, P.G., and Coates, K.D. 2002. Growth and crown morphological responses of boreal conifer seedlings and saplings with contrasting shade tolerance to a gradient of light and height. Can. J. For. Res. **32**(3): 458–468. doi:10.1139/x01-220.

Dabros, A., James Hammond, H.E., Pinzon, J., Pinno, B., and Langor, D. 2017. Edge influence of low-impact seismic lines for oil exploration on upland forest vegetation in northern Alberta (Canada). For. Ecol. Manage. **400**: 278–288. doi:10.1016/j.foreco.2017.06.030.

Dabros, A., Pyper, M., and Castilla, G. 2018. Seismic lines in the boreal and arctic ecosystems of North America: environmental impacts, challenges, and opportunities. Environ. Rev. **26**(2): 214–229. doi:10.1139/er-2017-0080.

Deane, P.J., Wilkinson, S.L., Moore, P.A., and Waddington, J.M. 2020. Seismic lines in treed boreal peatlands as analogs for wildfire fuel modification treatments. Fire, **3**(2): 21. doi:10.3390/fire3020021.

Debouk, H., Riera-Tatché, R., and Vega-García, C. 2013. Assessing post-fire regeneration in a Mediterranean mixed forest using lidar data and Artificial Neural Networks. Photogramm. Eng. Remote Sens. **79**(12): 1121–1130. doi:10.14358/PERS.79.12.1121.

De Groot, W.J., Bothwell, P.M., Taylor, S.W., Wotton, B.M., Stocks, B.J., and Alexander, M.E. 2004. Jack pine regeneration and crown fires. Can. J. For. Res. **34**(8): 1634–1641. doi:10.1139/x04-073.

DeLancey, E.R., Kariyeva, J., Bried, J.T., and Hird, J.N. 2019. Large-scale probabilistic identification of boreal peatlands using Google Earth Engine, open-access satellite data, and machine learning. PLoS One, **14**(6): e0218165. doi:10.1371/journal.pone.0218165. PMID:31206528.

DeMars, C.A., and Boutin, S. 2018. Nowhere to hide: effects of linear features on predator–prey dynamics in a large mammal system. J. Anim. Ecol. **87**(1): 274–284. doi:10.1111/1365-2656.12760.

Drake, J.B., Dubayah, R.O., Clark, D.B., Knox, R.G., Blair, J.B., Hofton, M.A., Chazdon, R.L., Weishampel, J.F., and Prince, S.D. 2002. Estimation of tropical forest structural characteristics, using large-footprint lidar. Remote Sens. Environ. **79**(2–3): 305–319. doi:10.1016/S0034-4257(01)00281-4.

Echiverri, L.F.I., Macdonald, S.E., and Nielsen, S.E. 2020. Disturbing to restore? Effects of mounding on understory communities on seismic lines in treed peatlands. Can. J. For. Res. **50**(12): 1340–1351. doi:10.1139/cjfr-2020-0092..

Ecological Stratification Working Group (ESWG). 1996. A National Ecological Framework for Canada. Agriculture and Agri-Food Canada and Environment Canada, Ottawa, ON, Canada. Cat. No. A42-65/1996E.

Elmqvist, T., Folke, C., Nyström, M., Peterson, G., Bengtsson, J., Walker, B., and Norberg, J. 2003. Response diversity, ecosystem change, and resilience. Front. Ecol. Environ. **1**(9): 488–494. doi:10.1890/1540-9295(2003)001[0488:RDECAR]2.0.CO;2.

Farr, T.G., Rosen, P.A., Caro, E., Crippen, R., Duren, R., Hensley, S., et al. 2007. The shuttle radar topography mission: Rev. Geophy. **45**: RG2004. doi:10.1029/2005RG000183.

Fenton, M.M., Waters, E.J., Pawley, S.M., Atkinson, N., Utting, D.J., and Mckay, K. 2013. Surficial geology of Alberta; Alberta Energy Regulator, AER/AGS Map 601, scale 1:1 000 000.

Filicetti, A.T., and Nielsen, S.E. 2018. Fire and forest recovery on seismic lines in sandy upland jack pine (*Pinus banksiana*) forests. For. Ecol. Manage. **421**: 32–39. doi:10.1016/j.foreco.2018.01.027.

Filicetti, A.T., and Nielsen, S.E. 2020. Tree regeneration on industrial linear disturbances in treed peatlands is hastened by wildfire and delayed by loss of microtopography. Can. J. For. Res. **50**: 936–945. doi:10.1139/cjfr-2019-0451.

Finnegan, L., MacNearney, D., and Pigeon, K.E. 2018*a*. Divergent patterns of understory forage growth after seismic line exploration: implications for caribou habitat restoration. For. Ecol. Manage. **409**: 634–652. doi:10.1016/j.foreco.2017.12.010.

Finnegan, L., Pigeon, K., Cranston, J., Hebblewhite, M., Musiani, M., Neufeld, L., et al. 2018*b*. Natural regeneration on seismic lines influences movement behaviour of wolves and grizzly bears. PLoS One, **13**(4): e0195480. doi:10.1371/journal.pone.0195480.

Finnegan, L., Pigeon, K.E., and MacNearney, D. 2019. Predicting patterns of vegetation recovery on seismic lines: Informing restoration based on understory species composition and growth. For. Ecol. Manage. **446**: 175–192. doi:10.1016/j.foreco.2019.05.026.

Fromm, M., Schubert, M., Castilla, G., Linke, J., and McDermid, G. 2019. Automated detection of conifer seedlings in drone imagery using convolutional neural networks. Remote Sens. **11**: 2585. doi:10.3390/rs11212585.

Greene, D.F., Zasada, J.C., Sirois, L., Kneeshaw, D., Morin, H., Charron, I., and Simard, M.J. 1999. A review of the regeneration dynamics of North American boreal forest tree species. Can. J. For. Res. **29**(6): 824–839. doi:10.1139/x98-112.

Grier, C.C. 1975. Wildfire effects on nutrient distribution and leaching in a coniferous ecosystem. Can. J. For. Res. **5**(4): 599–607. doi:10.1139/x75-087.

Honnay, O., Verheyen, K., and Hermy, M. 2002. Permeability of ancient forest edges for weedy plant species invasion. For. Ecol. Manage. **161**(1–3): 109–122. doi:10.1016/S0378-1127(01)00490-X.

Ilisson, T., and Chen, H.Y.H. 2009. The direct regeneration hypothesis in northern forests. J. Veg. Sci. **20**(4): 735–744. doi:10.1111/j.1654-1103.2009.01066.x.

Johnstone, J.F., and Chapin, F.S.I. 2006. Effects of soil burn severity on post-fire tree recruitment in boreal forest. Ecosystems, **9**(1): 14–31. doi:10.1007/s10021-004-0042-x.

Johnstone, J.F., Chapin Iii, F.S., Foote, J., Kemmett, S., Price, K., and Viereck, L. 2004. Decadal observations of tree regeneration following fire in boreal forests. Can. J. For. Res. **34**(2): 267–273. doi:10.1139/x03-183.

Johnstone, J.F., Celis, G., Chapin, F.S., Hollingsworth, T.N., Jean, M., and Mack, M.C. 2020. Factors shaping alternate successional trajectories in burned black spruce forests of Alaska. Ecosphere, **11**(5): e03129. doi:10.1002/ecs2.3129.

Key, C.H., and Benson, N.C. 2006. Landscape assessment: Remote sensing of severity, the Normalized Burn Ratio. FIREMON Fire Eff. Monit. Invent. Syst. Gen. Tech. Report, RMRS-GTR-164-CD: 305–325. doi:10.1002/app.1994.070541203.

Latham, A.D.M., Latham, M.C., Boyce, M.S., and Boutin, S. 2011. Movement responses by wolves to industrial linear features and their effect on woodland caribou in northeastern Alberta. Ecol. Appl. **21**(8): 2854–2865. doi:10.1890/11-0666.1.

Lee, P., and Boutin, S. 2006. Persistence and developmental transition of wide seismic lines in the western Boreal Plains of Canada. J. Env. Manag. **78**(3): 240–250. doi:10.1016/j.jenvman.2005.03.016.

McGaughey, R.J. 2009. FUSION/LDV: Software for LIDAR data analysis and visualization. US Dep. Agric. For. Serv. Pacific Northwest Res. Stn. Seattle, WA, U.S.A. 123(2).

Næsset, E., Gobakken, T., Holmgren, J., Hyyppä, H., Hyyppä, J., Maltamo, M., et al. 2004. Laser scanning of forest resources: The Nordic experience. Scand. J. For. Res. **19**(6): 482–499. doi:10.1080/02827580410019553.

Natural Resources Canada. 2019. Transport Networks in Canada — CanVec Series — Transport Features. Available from open.canada.ca/data/en/dataset/2dac78ba-8543-48a6-8f07-faeef56f9895 [accessed 12 December 2017].

Parks, S.A., Dillon, G.K., and Miller, C. 2014. A new metric for quantifying burn severity: The relativized burn ratio. Remote Sens. **6**(3): 1827–1844. doi:10.3390/rs6031827.

Pennock, D.J., and Sanborn, P. 2015. Soil Genesis and Geographical Distribution. Field Handbook for the Soils of Western Canada. Canadian Society of Soil Science. Canadian Society of Soil Science.

Pigeon, K.E., Anderson, M., MacNearney, D., Cranston, J., Stenhouse, G., and Finnegan, L. 2016. Toward the restoration of caribou habitat: understanding factors associated with human motorized use of legacy seismic lines. Environ. Manage. **58**(5): 821–832. doi:10.1007/s00267-016-0763-6.

Pinzon, J., Dabros, A., Riva, F., and Glasier, J.R.N. 2021. Short-term effects of wildfire in boreal peatlands: does fire mitigate the linear footprint of oil and gas exploration? Ecol. Appl. **31**: e02281. doi:10.1002/eap.2281.

QGIS.org. 2019. QGIS 3.10. QGIS Geographic Information System. QGIS Association. Available from http://www.qgis.org.

R Core Team. 2020. R: A language and environment for statistical computing. R Foundation for Statistical Computing, Vienna, Austria. Available from https://www.R-project.org/ [accessed 11 August 2020].

Revel, R.D., Dougherty, T.D., and Downing, D.J. 1984. Forest growth & revegetation along seismic lines. University of Calgary Press, Calgary, Alberta, United States. Available from https://www.osti.gov/servlets/purl/6109132.

Riva, F., Acorn, J.H., and Nielsen, S.E. 2018. Localized disturbances from oil sands developments increase butterfly diversity and abundance in Alberta's boreal forests. Biol. Conserv. **217**: 173–180. doi:10.1016/j.biocon.2017.10.022.

Riva, F., Pinzon, J., Acorn, J.H., and Nielsen, S.E. 2020. Composite effects of cutlines and wildfire result in fire refuges for plants and butterflies in boreal treed peatlands. Ecosystems, **23**(3): 485–497. doi:10.1007/s10021-019-00417-2.

Stevenson, C.J., Filicetti, A.T., and Nielsen, S.E. 2019. High precision altimeter demonstrates simplification and depression of microtopography on seismic lines in treed peatlands. Forests, **10**(4): 295. doi:10.3390/f10040295.

Stocks, B.J., Mason, J.A., Todd, J.B., Bosch, E.M., Wotton, B.M., Amiro, B.D., et al. 2002. Large forest fires in Canada, 1959–1997. J. Geophys. Res. **108**(D1): 8149. doi:10.1029/2001JD000484.

Tymstra, C., MacGregor, B., and Mayer, B. 2002. Alberta's House River Fire. Fire Manag. Today, **65**(1): 16–18.

Tymstra, C., Rogeau, M.-P., and Wang, D. 2005. Wildfire Science and Technology Report PFFC-01-05. Alberta wildfire regime analysis. Alberta Sustainable Resource Development, Forest Protection Division, Wildfire Policy and Business Planning Branch, Edmonton, Alberta. doi:10.5962/bhl.title.113828.

van Rensen, C.K., Nielsen, S., White, B., Vinge, T., and Lieffers, V.J. 2015. Natural regeneration of forest vegetation on legacy seismic lines in boreal habitats in Alberta's oil sands region. Biol. Conserv. **184**: 127–135. doi:10.1016/j.biocon.2015.01.020.

Vastaranta, M., Holopainen, M., Yu, X., Haapanen, R., Melkas, T., Hyyppä, J., and Hyyppä, H. 2011. Individual tree detection and area-based approach in retrieval of forest inventory characteristics from low-pulse airborne laser scanning data. Photogramm. J. Finl. **22**(2): 1–13.

Whitman, E., Parisien, M.A., Thompson, D.K., Hall, R.J., Skakun, R.S., and Flannigan, M.D. 2018. Variability and drivers of burn severity in the northwestern Canadian boreal forest: Ecosphere, **9**: e02128. doi:10.1002/ecs2.2128.

Whitman, E., Parisien, M.-A., Holsinger, L.M., Park, J., and Parks, S.A. 2020. A method for creating a burn severity atlas from fire perimeters: an example from Alberta, Canada. Int. J. Wildl. Fire. **29**: 995–1008. doi:10.1071/WF19177.

Wulder, M.A., Bater, C.W., Coops, N.C., Hilker, T., and White, J.C. 2008. The role of LiDAR in sustainable forest management. For. Chron. **84**(6): 807–826. doi:10.5558/tfc84807-6.

Appendices A and B appear on the pages that follow.

Appendix A

Table A1. Data sources and description.

Data type	Source	Description
ALS point cloud	Government of Alberta ALS point cloud database	Collected approximately 2007–2009 at a mean point cloud density of 1.4 returns·m^{-2}. Vertical accuracy is approximately ±0.30 m, horizontal accuracy is approximately ±0.45 m.
Cutblocks	Landsat satellite imagery	Cutblocks were identified using a Canada-wide Landsat-based 30 m resolution change-detection dataset (Guindon et al. 2018).
Seismic line shapefiles	Human Footprint Inventory (ABMI 2018*a*)	Maps human footprint features across the entire province of Alberta, based on spatial data from a variety of organizations and manual interpretation of remotely sensed imagery.
Fire perimeters	Canadian National Fire Database (Canadian Forest Service 2015)	National-scale collection of forest fire data from various Canadian fire management agencies, including data from field personnel, photo interpreters, satellite imagery, and other sources.
Fire severity	Google Earth Engine	Differenced normalized burn ratio (dNBR) was calculated from pre- and post-fire Landsat satellite imagery (Whitman et al. 2020).
Roads shapefile	Natural Resources Canada National Roads Network	Road map shapefiles produced, updated, and distributed through Natural Resources Canada, Statistics Canada, and provincial and territorial governments (Natural Resources Canada 2019).
Water bodies shapefile	Boreal Surface Water Inventory (ABMI 2018*b*)	Surface water polygons derived from a machine learning algorithm based on Sentintel-1 and -2 satellites, subset into permanent and recurring water bodies. For specific information see DeLancey et al. (2018).
Aerial photography	Bing Maps (Microsoft 2019)	Aerial photography imagery.
Wetland inventory	Boreal Wetland Probability Dataset (ABMI 2019)	Map of lowland and upland areas, generated using a machine learning framework on optical satellite data (Sentinel-2), Synthetic Aperture Radar (Sentinel-1), and elevation. Accuracy of approximately 83% (DeLancey et al. 2019).

Table A2. Summary (median ± standard deviation) of airborne laser scanning return statistics by plot class, for burned plots.

	Upland (n = 419)			Lowland (n = 645)		
	Seismic line	Control	p value	Seismic line	Control	p value
$Height_{P05}$ (m)	0.16±0.03	0.16±0.54	0.0001	0.15±0.01	0.15±0.01	0.0006
$Height_{P10}$ (m)	0.18±0.08	0.19±0.95	<0.0001	0.16±0.02	0.16±0.12	<0.0001
$Height_{P25}$ (m)	0.24±0.89	0.27±2	<0.0001	0.18±0.15	0.19±0.33	<0.0001
$Height_{P50}$ (m)	0.49±1.89	0.75±3.15	<0.0001	0.26±0.61	0.30±1.06	<0.0001
$Height_{P75}$ (m)	1.57±3.16	2.31±4.38	<0.0001	0.49±1.55	1.05±2.17	<0.0001
$Height_{P95}$ (m)	5.30±5.45	10.36±5.62	<0.0001	3.38±3.21	5.75±3.47	<0.0001
$Height_{P99}$ (m)	10.97±6.03	13.87±5.65	<0.0001	5.93±3.94	7.87±3.86	<0.0001
$Height_{mean}$ (m)	1.43±1.81	2.34±2.69	<0.0001	0.76±0.84	1.30±1.12	<0.0001
$Height_{variance}$	4.76±11.68	11.27±13.2	<0.0001	1.69±3.94	4.01±5.55	<0.0001
$Height_{kurtosis}$	9.31±19.2	6.39±20.75	<0.0001	8.13±36.56	5.70±20.69	<0.0001
$Height_{skewness}$	2.50±1.91	1.95±2.08	<0.0001	2.41±2.50	1.86±2.00	<0.0001
Canopy relief ratio	0.12±0.09	0.15±0.12	<0.0001	0.11±0.08	0.13±0.08	<0.0001
% $returns_{>0.15\ m}$	50.18±23.18	55.95±19.57	<0.0001	28.37±18.87	34.08±17.69	<0.0001
% $returns_{0.15–2.0\ m}$	36.55±17.26	34.68±16.47	0.4579	23.59±16.92	25.48±14.52	0.0007
% $returns_{2.0–5.0\ m}$	3.19±11.18	4.94±10.72	0.0063	1.04±4.01	2.56±5.64	<0.0001
% $returns_{5.0–10.0\ m}$	1.17±5.09	3.24±7.98	<0.0001	0.53±3.06	2.11±4.98	<0.0001
% $returns_{10.0–30.0\ m}$	0.74±6.63	2.95±12.19	<0.0001	0.00±0.91	0.00±2.07	<0.0001
% $returns_{>\ 2.0\ m}$	7.47±15.86	15.05±20.26	<0.0001	1.89±6.65	5.95±10.27	<0.0001

Note: The p values are from paired Wilcoxon rank-sum tests.

Table A3. Difference (m) in vegetation height between seismic lines and control plots, calculated from $Height_{P99}$, including upland and lowland plots.

Fire	Lowland class	Control – seismic line difference (m)
Burned	Lowland	1.65±4.25
	Upland	1.69±5.70
Unburned	Lowland	0.77±2.96
	Upland	0.92±4.63

Table A4. Independent model variables in order of importance (0–100) to the burned site model.

Variable	Descriptor
UPLAND	Upland–lowland class, as estimated from the ABMI Boreal Wetland Probability dataset (DeLancey et al. 2019).
SEISMIC	Seismic line site (1) or control forest site (0).
CTI	Compound topographic index, calculated from a 15 m resolution ALS-derived digital elevation model.
dNBR	Differenced normalized burn ratio (dNBR, Key and Benson 2006), a measure of fire severity, calculated from pre- and post-fire Landsat satellite imagery (Whitman et al. 2020).
ROADDIST	Distance to roads, calculated from the Natural Resources Canada CanVec Transportation dataset (Natural Resources Canada 2019).

Fig. A1. Airborne laser scanning canopy height model for two lowlands in Chisolm (A) and House River (B). Green areas represent treed lowlands, while areas devoid of trees represent shrubby lowlands. Linear disturbances are seismic lines. Canopy height model was calculated at a 2 m × 2 m resolution. Inset basemap is a hillshade of the NASA SRTM 30 m digital elevation model (Farr et al. 2007). Produced in QGIS 3.10 (QGIS.org 2019). [Colour online.]

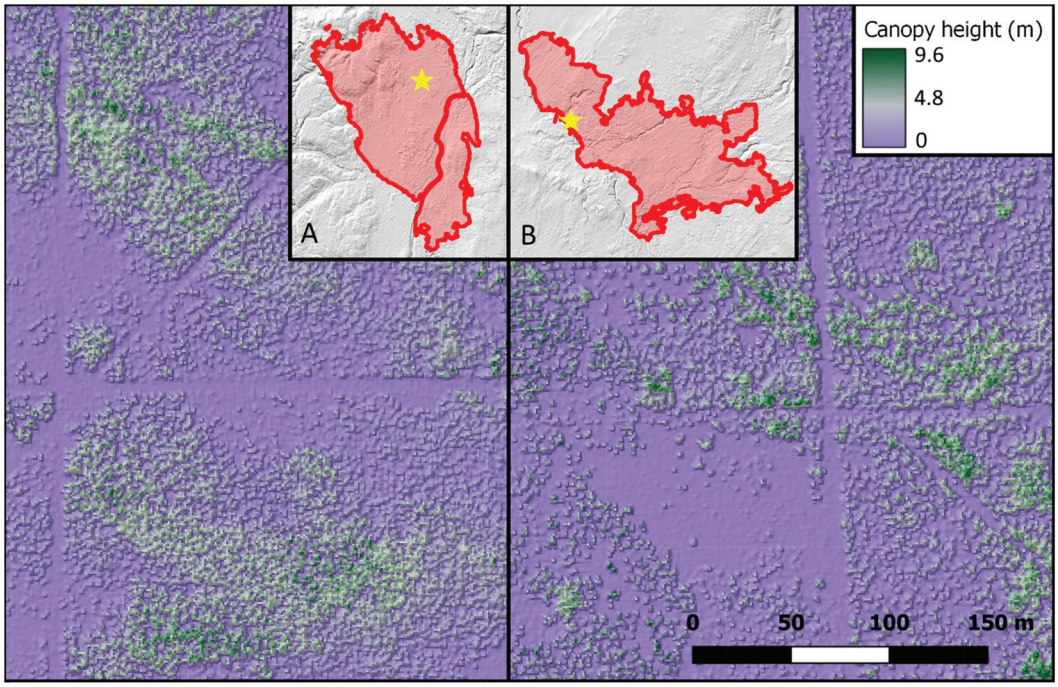

Fig. A2. Comparison of selected airborne laser scanning statistics from unburned areas, between seismic lines and paired control plots (n = 1006), grouped by upland (orange) and lowland (blue). Boxes represent the 25th, 50th, and 75th percentiles (quartiles). Whiskers represent the lowest (highest) datum within 1.5 times the interquartile range (third - first quartile) of the first (third) quartile. All comparisons between seismic lines and controls are statistically significant (paired Wilcoxon rank-sum test, $p < 0.0001$). [Colour online.]

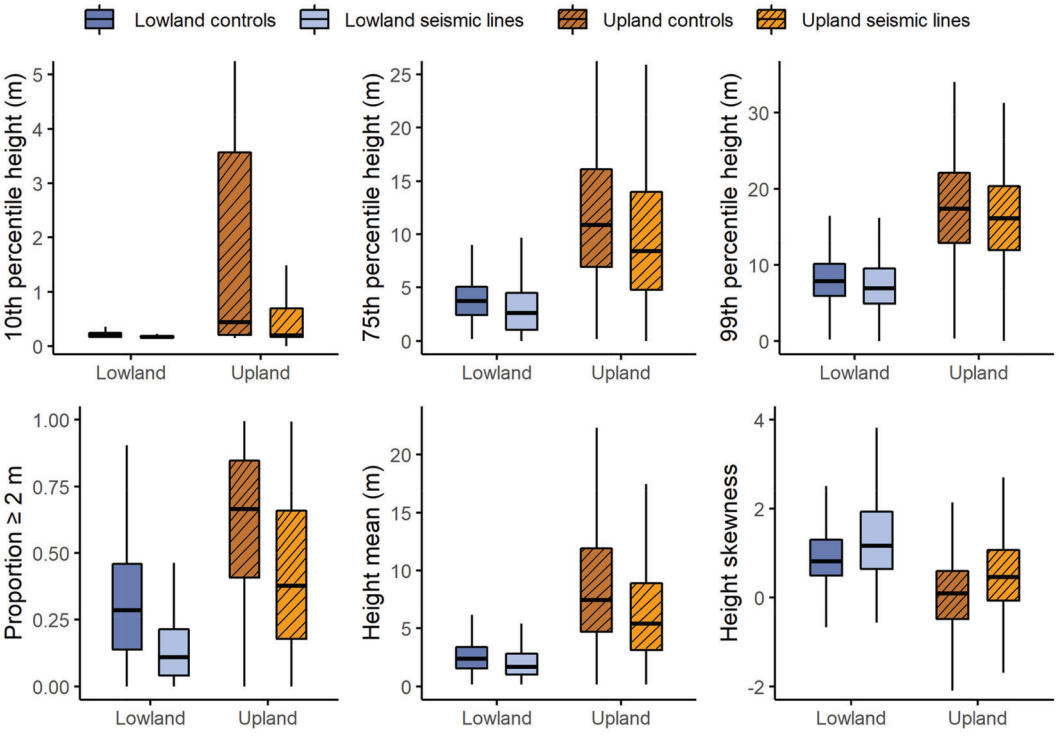

Fig. A3. Seismic lines only, comparing selected airborne laser scanning statistics between burned and unburned plots (n = 2070), grouped by upland (green) and lowland (pink). Boxes represent the 25th, 50th, and 75th percentiles, and whiskers represent the interquartile range ×1.5. [Colour online.]

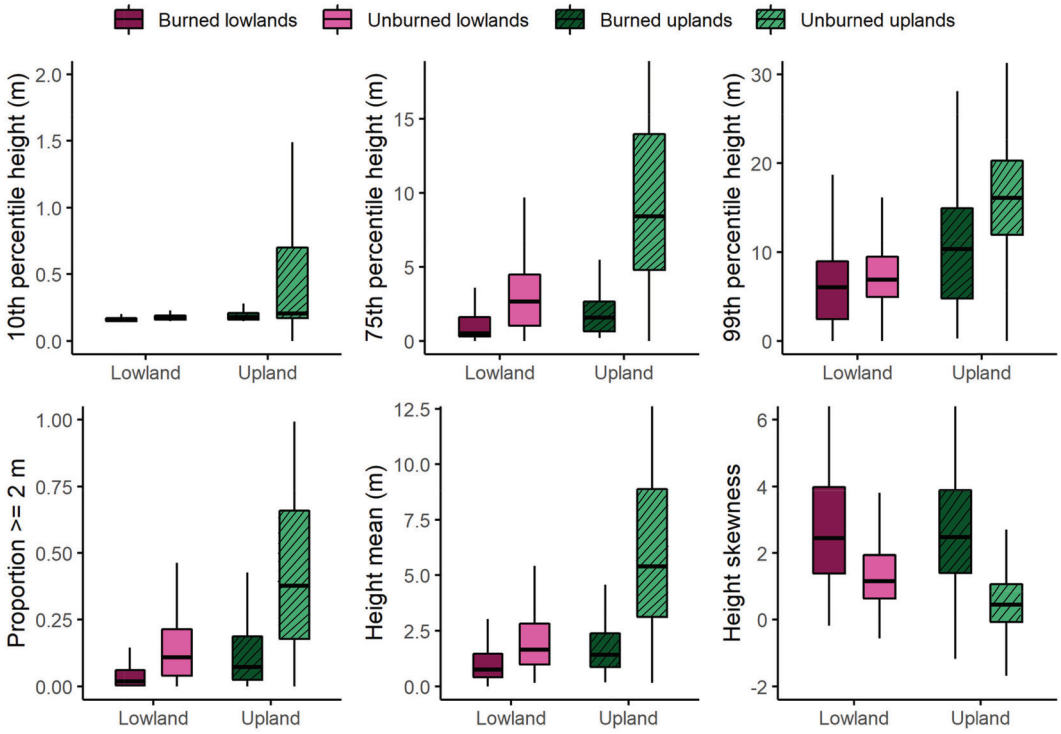

Fig. A4. Paired plot difference (burned seismic line – burned control plot) for six airborne laser scanning statistics, grouped by upland (orange) and lowland (blue), showing only burned plots (n = 1064). Boxes represent the 25th, 50th, and 75th percentiles, and whiskers represent the interquartile range ×1.5. [Colour online.]

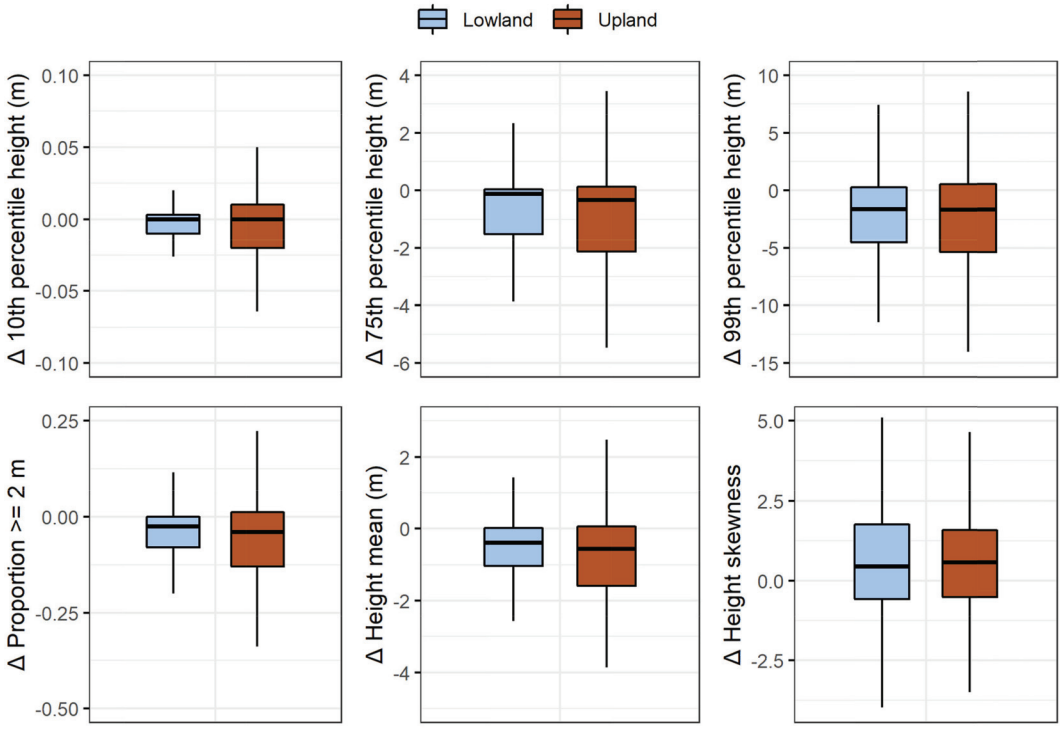

References

ABMI. 2018*a*. Wall-to-Wall Human Footprint Inventory. Alberta Biodiversity Monitoring Institute and Alberta Human Footprint Monitoring Program, Edmonton, AB. Available from https://abmi.ca/home/data-analytics/da-top/da-product-overview/Advanced-Landcover-Prediction-and-Habitat-Assessment–ALPHA–Products/Boreal-Surface-Water-Inventory.html [accessed 31 October 2019].

ABMI. 2018*b*. Boreal Surface Water Inventory. Available from https://abmi.ca/home/data-analytics/da-top/da-product-overview/Advanced-Landcover-Prediction-and-Habitat-Assessment–ALPHA–Products/Boreal-Surface-Water-Inventory.html [accessed 20 December 2018].

ABMI. 2019. Boreal Wetland Probability Data. Available from https://abmi.ca/home/data-analytics/da-top/da-product-overview/Advanced-Landcover-Prediction-and-Habitat-Assessment—ALPHA—Products/Boreal-Wetland-Probability-Data.html?scroll=true [accessed 20 December 2018].

Canadian Forest Service. 2015. Canadian National Fire Database—agency fire data. Natural Resources Canada, Canadian Forest Service, Northern Forestry Centre, Edmonton, Alberta. Available from http://cwfis.cfs.nrcan.gc.ca/en_CA/nfdb [accessed 12 March 2018].

DeLancey, E.R., Kariyeva, J., Cranston, J., and Brisco, B. 2018. Monitoring hydro temporal variability in Alberta, Canada with Multi-Temporal Sentinel-1 SAR Data. Can. J. Remote Sens. **44**(1): 1–10. doi:10.1080/07038992.2018.1417734.

DeLancey, E.R., Kariyeva, J., Bried, J.T., and Hird, J.N. 2019. Large-scale probabilistic identification of boreal peatlands using Google Earth Engine, open-access satellite data, and machine learning. PLoS One, **14**(6): e0218165. doi:10.1371/journal.pone.0218165. PMID:31206528.

Farr, T.G., Rosen, P.A., Caro, E., Crippen, R., Duren, R., Hensley, S., et al. 2007. The shuttle radar topography mission: Rev. Geophys. **45**: RG2004. doi:10.1029/2005RG000183.

Guindon, L., Bernier, P., Gauthier, S., Stinson, G., Villemaire, P., and Beaudoin, A. 2018. Missing forest cover gains in boreal forests explained. Ecosphere, **9**: e02094. doi:10.1002/ecs2.2094.

Key, C.H., and Benson, N.C. 2006. Landscape assessment: Remote sensing of severity, the Normalized Burn Ratio. FIREMON Fire Eff. Monit. Invent. Syst. Gen. Tech. Report, RMRS-GTR-164-CD: 305–325. doi:10.1002/app.1994.070541203.

Microsoft. 2019. Bing Maps. https://www.bing.com/maps [accessed 31 October 2019].

Natural Resources Canada. 2019. Transport Networks in Canada - CanVec Series - Transport Features. Available from open.canada.ca/data/en/dataset/2dac78ba-8543-48a6-8f07-faeef56f9895. [accessed 12 December 2017].

QGIS.org. 2019. QGIS 3.10. QGIS Geographic Information System. QGIS Association. Available from http://www.qgis.org.

Whitman, E., Parisien, M.-A., Holsinger, L.M., Park, J., and Parks, S.A. 2020. A method for creating a burn severity atlas from fire perimeters: an example from Alberta. Canada. Int. J. Wildl. Fire. doi:10.1071/WF19177.

Appendix B

We randomly generated sample plots and control plots from the 2016 Alberta Biodiversity Monitoring Institute (ABMI) Human Footprint Inventory (ABMI 2018). This dataset was originally validated using SPOT6 satellite imagery as part of the Alberta Human Footprint Monitoring Program (https://abmi.ca/home/data-analytics/da-top/da-product-overview/Human-Footprint-Products/HF-inventory.html). We performed visual validation of on a subset of our randomly generated seismic line plots using Bing Aerial Imagery (https://www.bing.com/maps; Microsoft 2019. This was done to assess the accuracy of the ABMI Human Footprint Inventory, which may have included erroneously identified low-impact seismic lines, pipelines, roads, or other features. We assessed 400 seismic line plots, including 100 from within each of the Chisholm and House River fires, and 100 from within 20 km of each of the fire perimeters. We found that approximately 97% of our plots were correctly located on what appeared to be conventional seismic lines, with the remainder located on water features or industrial features (Appendix Table B1). Some of these features may have been converted from seismic lines later than the ALS collection, making this a conservative estimate.

Table B1. Aerial identification of a subset of 400 seismic line plots, with 97% appearing to be seismic lines and not misidentified industrial features.

Feature type	*n*
Seismic line	387
Pipeline	3
Road	1
Water	5
Wellpad	3
Industrial facility	1

The construction date of seismic lines likely impacts regeneration success, and the possibility that seismic line construction occurred after wildfire represents a source of uncertainty in our study. The Human Footprint Inventory (ABMI 2018) includes "YEAR" as an attribute, indicating the year the seismic line was first observed in the remote sensing imagery. However, 79% of our plots are missing this attribute, likely due to their construction occurring prior to the availability of remote sensing imagery. Based on an analysis of those plots with a "YEAR" attribute, we conclude that it is likely that only a small fraction of our seismic line plots were constructed after the wildfire occurred (Appendix Fig. B1). The dataset also retains a feature when that feature disappears from the landscape, which should limit the number of regenerated seismic lines missed in our analysis, provided that they were included in the Government of Alberta spatial records of seismic line construction or the interpreted remote sensing record.

Fig. B1. Date of remote sensing imagery when seismic line plots were first observed in the ABMI Human Footprint Inventory (ABMI 2018). Vertical lines indicate the wildfire year. Of 1335 plots, 1051 plots had no observation date listed, indicating that construction probably pre-dated the availability of remote imagery. [Colour online.]

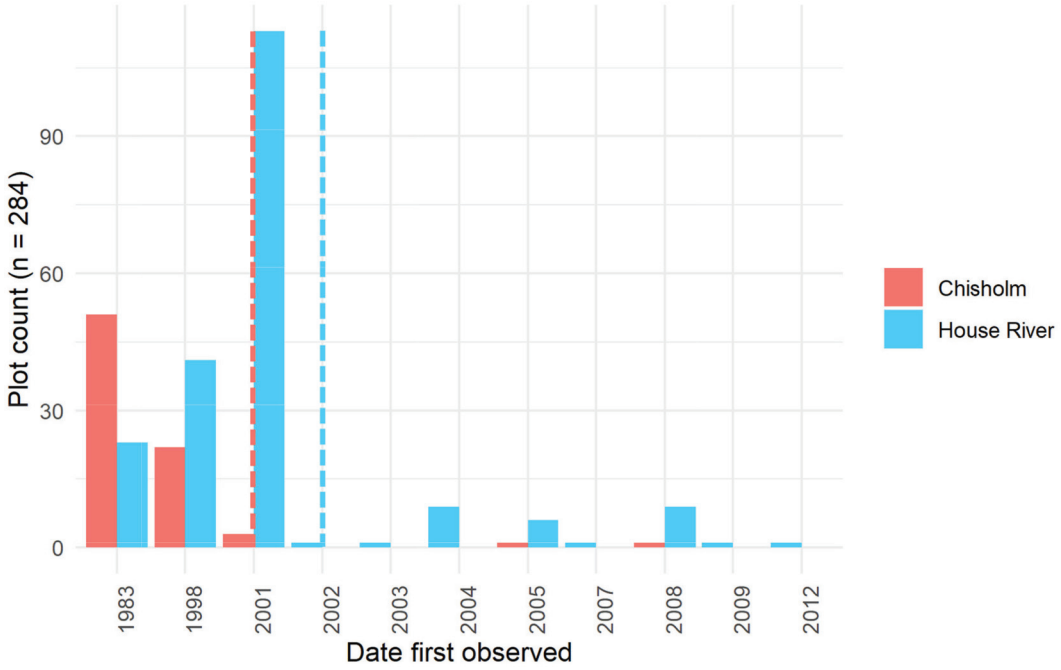

References

ABMI. 2018. Human Footprint Inventory Wall-to-Wall Human Footprint Inventory. Alberta Biodiversity Monitoring Institute and Alberta Human Footprint Monitoring Program, Edmonton, AB. Available from https://www.abmi.ca/home/data-analytics/da-top/da-product-overview/Human-Footprint-Products/HF-inventory.html [accessed 31 October 2019].

Microsoft. 2019. Bing Maps. Available from https://www.bing.com/maps [accessed 31 October 2019].